Nature Environment and Pollution Technology
An International Quarterly Scientific Journal

p-ISSN: 0972-6268
(Print copies up to 2016)
e-ISSN: 2395-3454

Vol. 22 | No. 3 | pp. 1481-1491 | 2023

Original Research Paper

https://doi.org/10.46488/NEPT.2023.v22i03.033

Open Access Journal

Artificial Neural Network Modeling for Adsorption Efficiency of Cr(VI) Ion from Aqueous Solution Using Waste Tire Activated Carbon

Gaurav Meena† and Nekram Rawal
Department of Civil Engineering, Motilal Nehru National Institute of Technology, Allahabad, Prayagraj, India
†Corresponding author: Gaurav Meena; gaurav.jpid@gmail.com

Nat. Env. & Poll. Tech.
Website: www.neptjournal.com

Received: 28-01-2023
Revised: 29-03-2023
Accepted: 05-04-2023

Key Words:
Artificial neuron network
RMSE
MAE
Waste tires
Activated carbon

ABSTRACT

In this study, waste tires were used to develop activated carbon for the adsorption of Cr(VI) from aqueous solutions, and an artificial neural network (ANN) model was applied to predict the adsorption efficiency of waste-tire activated carbon (WTAC). SEM and FTIR were used to characterize the developed WTAC. A three-layer ANN with different training algorithms and hidden layers with different numbers of neurons was developed using 79 data sets gathered from batch adsorption experiments with different initial Cr(VI) ion concentrations, contact periods, temperatures, and doses. Conjugate gradient backpropagation of Powell-Beale restarts (traincgb) was found to be the best training algorithm among all the training algorithms, with an RMSE of 5.894 and an R^2 of 0.985. The ANN topology had 4, 8, and 4 neurons in the input, hidden, and output layers. The correlation coefficient of the ANN models of Cr(VI) ion adsorption efficiency is 0.977.

INTRODUCTION

Heavy metal water contamination is a major issue everywhere in the world (Dodbiba et al. 2015, Veglio & Beolchini 1997). Chromium is also significant in water contamination because tons of chromite ore is generated annually worldwide. Ferro chromite is created through the direct decrease of the ore, whereas Cr metal is created through the aluminothermic process, chrome alum solutions, or electrolysis of CrO_3. The production of chromate, electroplating, leather tanning, metal polishing, and chromate preparation are only a few industries that make substantial use of chromium and its derivatives (Kowalski 1994). Chromium predominantly appears in two oxidation states in aqueous solutions: trivalent chromium and hexavalent chromium. The hexavalent form of chromium is hazardous, can cause cancer, and can also mutate DNA. For instance, lung cancer has been associated with $Cr_2O_7^{2-}$ (El-Sikaily et al. 2007, Li 2008).

One of the main factors contributing to the importance of chromium (III) and chromium (VI) to the environment is their stability in their native habitats. Due to its high water solubility, mobility, and simplicity of reduction, Cr(VI) is 100 times more dangerous than Cr (III) (Gómez & Callao 2006). The fundamental causes of Cr(VI) toxicological effects are its oxidizing capabilities and the subsequent formation of free radicals during its intracellular reduction to Cr (III) (Das 2004). The World Health Organization (WHO 2020) recommends a chromium (VI) wastewater toxicity limit of 0.05 $mg.L^{-1}$ with a combined maximum permitted discharge of 2.0 $mg.L^{-1}$ (WHO 2020).

Chromium may be removed from wastewater produced in various industrial settings using several methods. Here are a few instances that exist. Some examples of these processes are reduction followed by chemical precipitation (Zhou 1993), ion exchange (Tiravanti et al. 1997), reduction; electrochemical precipitation (Kongsricharoern & Polprasert 1996); solvent extraction (Meegoda 2000); membrane separation (Chakravarti et al. 2000); evaporation (Aksu 1996); and foam separation (Jiao & Ding 2009). At low quantities, conventional approaches to chromium removal, such as those outlined above, are either prohibitively expensive or ineffective due to the element's solubility in water. In light of this, adsorption ought to be considered a workable alternative. As an adsorbent, commercial activated carbon, also known as CAC, is utilized to remove Cr (Selomulya et al. 1999), Cd (Kannan & Rengasamy 2005), Cu, Zn (Monser & Adhoum 2002) and Ni (Basso et al. 2002) from wastewater. However, commercial activated carbon intended exclusively for eliminating heavy metals can be fairly expensive. In the search for adsorbents that are both effective and economical, a great number of investigations have been carried out. In this research, a wide variety of

absorbents, such as starch xanthate (Religa et al. 2011), chitosan (Ngah et al. 2005), sawdust from *Pinus sylvestris* (Taty-Costodes et al. 2003), bagasse sugar (Gupta 2003), bentonite (Bereket et al. 1997), and old car tires (Rowley et al. 1984) were investigated.

The adsorption mechanism is very complicated, which makes it hard to model and simulate with traditional mathematical models. This is because a wider range of sorption process factors interacts, leading to nonlinear relationships. To ensure that every control measure is managed in the most effective manner possible, it is required to build a suitable model to achieve effective operation and design. A high-quality representative model may be of considerable assistance in optimizing the input parameters. ANNs have been applied to the fields of wastewater treatment (Chen & Kim 2006, Gontarski et al. 2000, Pai 2007, Qiao et al. 2020, Sahoo & Ray 2006), membrane processes (Fagundes-Klen 2007, Guadix et al. 2010, Libotean 2009, Prakash et al. 2008), and biosorption (Sadrzadeh et al. 2009, Yetilmezsoy & Demirel 2008) for prediction and simulation because of their reliability, robustness, and prominent features in picking up the non-linearity relation of variables in intricate systems. Heavy metal adsorption efficiency from water can be predicted using ANNs. However, the available data is scant (Kashaninejad et al. 2009). Therefore, this research aimed to find the best ANN structure and associated parameters for predicting the removal efficiency of activated carbon from waste tires of Cr(VI) ions in an aqueous solution.

MATERIALS AND METHODS

Materials

Analytical grade reagents were used in the study and purchased from Uma Scientific, Prayagraj. Stock Solutions

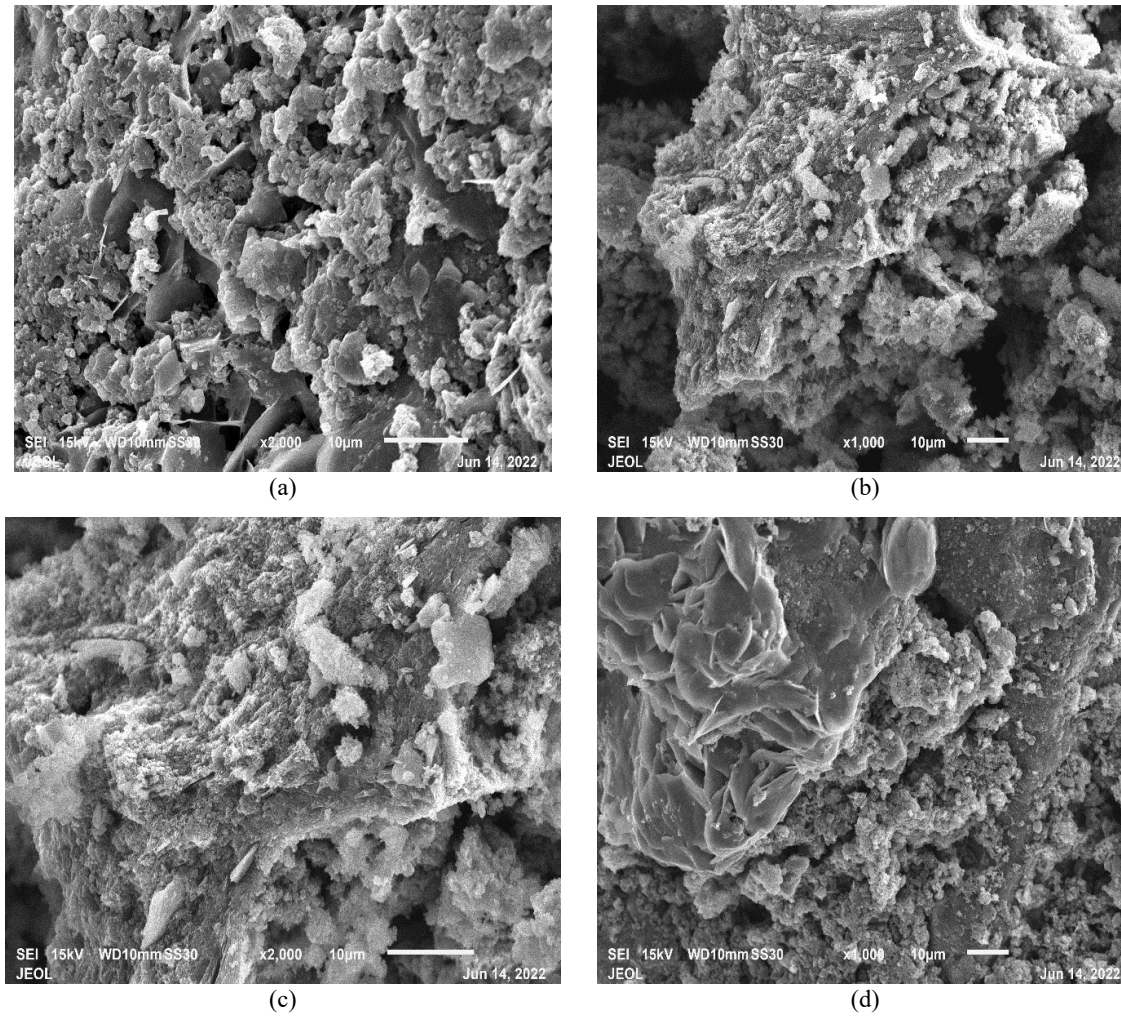

Fig. 1: SEM micrograph (a, b) before adsorption; (c, d) after adsorption.

and other solutions were prepared using a double-distillation unit. A stock solution of Cr(VI) was prepared using 144 mg Potassium dichromate ($K_2Cr_2O_7$) dissolved in 100 mL distilled water which gives 500 mg.L^{-1} Cr(VI). The artificial wastewater with the required Cr(VI) concentration used in the tests was made from a stock solution. Waste tires used during the study were sourced from a near tire repair shop. Fetched tires were cut into 10-12 mm pieces, and the dirt was cleaned by shocking in diluted HCl for 24 h, followed by two to three rinses with distilled water, and drying in a hot air oven at 100°C for 4 h. After cleaning and drying, waste tires were carbonized at 400°C for 4 h. Chemical and heat treatments of carbonized waste tires prepared the activated carbon. A weight ratio of 1:2 of carbonized tires to H_2SO_4 was initially poured into a 250 mL crucible to perform the chemical treatments. The mixture was then left to react for 4 h while being stirred intermittently throughout the reaction duration. After that, the items. After that, the mixture was heated at 400°C for one hour, and then, once the mixture had cooled, it was stored in a glass container.

Adsorbent Media Characterization

Scanning electron microscopy (SEM) was used to investigate the difference in surface morphology between the WTAC before and after the adsorption of the Cr(VI) ions. Fig. 1 (a-b) show the results of SEM imaging before adsorption at a different level of magnification, and Fig. 2 (c-d) shows the results after adsorption at different magnification. The irregular surface and presence of pores before adsorption could be assumed to be active sites for chromium uptake.

The sample's Fourier transform infrared (FTIR) was collected over a wide spectral range between 4000 and 400 cm^{-1} to collect high-resolution information. The critical features of FTIR spectra of the sample are shown in Fig. 2. The 3415.02 cm^{-1} peaks denoted the presence of a hydroxyl group, which might be carbon black surface groups or groups generated from the hydroxylation of oxides (Manchón-Vizuete 2005) chemical and combined (thermal and chemical or vice versa.

Batch Adsorption Experiments

Adsorption batch tests were conducted in a conical flask on a temperature-controlled orbital shaker. Aliquots of treated samples were filtered using grade 1 Whatman filter paper (pore size 11 μ) after adsorption. Colorimetric analysis using a spectrophotometer (LABINDIA UV 30000+) was used to determine chromium levels in the samples. The batch adsorption was done at different contact periods and with different chromium concentrations, times, and temperatures, as indicated by the statistics for the factor mentioned in Table 2. The following equation was used to calculate the adsorption capacities.

$$q_e = \frac{(C_0 - C_t)V}{m} \quad \ldots(1)$$

Where qe represents the adsorption capacity in mg.g^{-1}, Co represents the initial Cr concentration, Ct represents the Cr concentration at time t, V represents the volume of the solution in L, and m represents the mass of the adsorbent (g).

Artificial Neural Networks

Artificial neural networks (ANNs) have significant computational modeling power. Because of their adaptive structure, they can recognize complicated nonlinear relationships. This is especially true when the evident

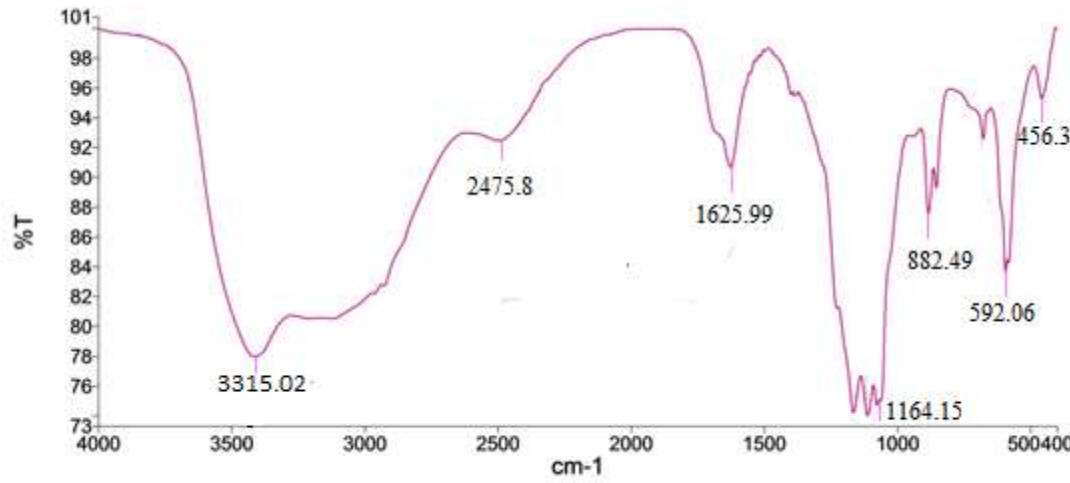

Fig. 2: FTIR spectra of activated carbon.

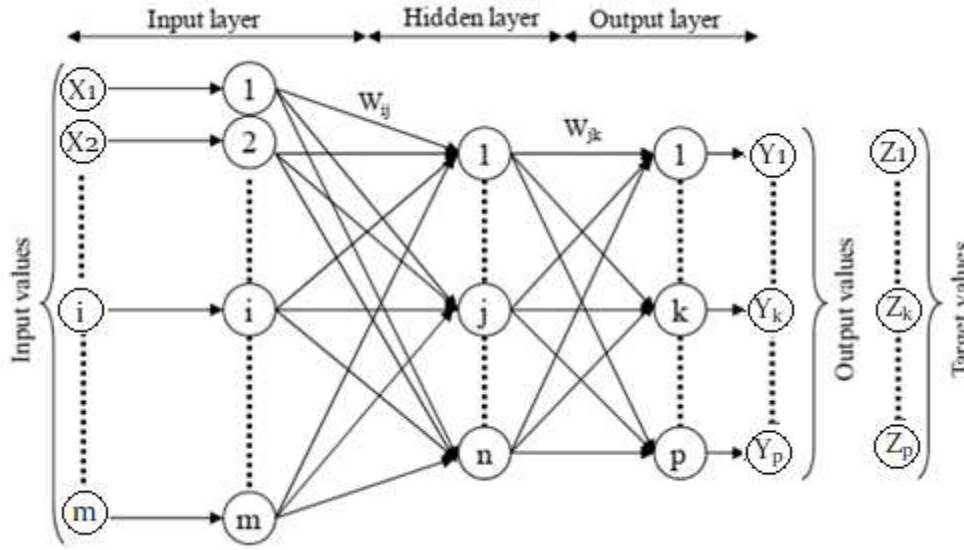

Fig. 3: ANN fundamental structure.

structure of the variable-variable relationship is ambiguous. The basic purpose of an ANN model is to solve any problem that cannot be solved using more traditional mathematical or statistical methodologies. Fig. 3 depicts an ANN's fundamental structure, consisting of three layers: an input layer with dependent variables, a hidden layer, and an output layer with dependent variables.

As shown in Fig. 3, each layer of a typical ANN consists of many strongly connected processing components called "neurons" or "nodes." In addition, all neurons except the output layer are linked to the sub-layer neurons by the connection strength (w value). The neurons in each layer get information from various sources, including the input layer's original data, the hidden layer's output from other nodes in the previous layer, and the output layer's original data. A line, which conveys information from one node to the following, represents the connectivity between neurons. Data is introduced into the network in the input layer, and the input is calculated in the hidden layer and output layer by weighing the total output obtained in the previous layer. This mechanism is driven by the "weights," or the degree of connectivity between two neurons. However, the inputs are transferred to the hidden and output layers using activation functions, which then compute the outputs of those layers. An activation function is a mathematical term for a nonlinear transfer function. Transfer functions that are among the most

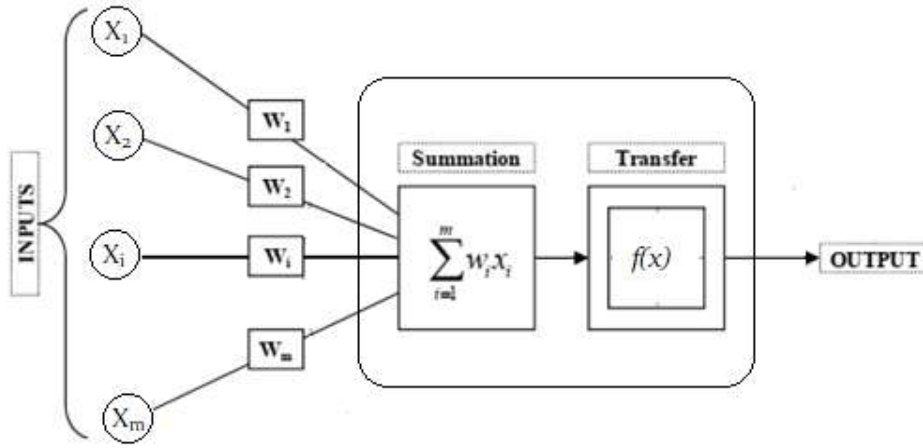

Fig. 4: Illustration of operation within a neuron.

common include the tangent sigmoid (tansig), logarithmic sigmoid (logsig), and linear (purelin). The mathematical descriptions of the logsig and tansig transfer functions are provided by equations (2) and (4), respectively, while equation (3) explains the purelin transfer function. The tansig transfer function provides the most accurate predictions compared to the other transfer functions.

$$f(x) = \frac{e^{x}-e^{-x}}{e^{x}+e^{-x}} \quad \ldots(2)$$

$$f(x) = \frac{1}{1+e^{-x}} \quad \ldots(3)$$

$$f(x) = x \quad \ldots(4)$$

Fig. 4 illustrates a flow that depicts the flow of information within a neuron. When the input is multiplied by its weight, the sum function applies to all inputs of the previous layer, as applied to the previous layer (w value). Then the neuron's output is determined by passing this unique value through the transfer function.

Collecting, analyzing, and processing data is the first step in the development of the ANN model, followed by training the network, testing the training network, selecting the model (determining the optimal structure of the ANN, training functions, training algorithms, and network parameters), and simulating and predicting using the training network. All ANN models developed in this study followed these steps.

In ANN, the training algorithm is a process for adjusting the parameters of a network until they are optimal for a given input-output transformation problem. No universally superior algorithm exists because performance varies greatly among problems of varying sizes, complexities, and data availability. Thus, 11 training algorithms from 6 different categories were compared and evaluated. Table 1 summarizes all the training algorithms and their functions.

Table 1: ANN training algorithms.

Training algorithm	function
Levenberg-Marquardt (LM)	trainlm
Gradient descent(GD) with a variable learning rate	traingdm
	traingda
	traingdx
Resilient backpropagation(RP)	trainrp
Conjugated gradient descent(CG)	traincgb
	traincgp
	trainscg
Quasi-Newton algorithm	trainoss
	trainbfg
Bayesian regularization	trainbr

Performance Assessment Criteria of the ANN Model

The reliability of the created ANN models was evaluated in four different methods: mean absolute error (MAE), root mean square error (RMSE), coefficient of determination (R^2)

The root-mean-squared error (RMSE) was used as a measure of the accuracy of the model, and it may be computed as follows:

$$RMSE = \sqrt{\frac{\sum_{i=1}^{n}(Y_{pre,i}-Y_{obs,i})}{n}} \quad \ldots(5)$$

$Y_{pre,i}$ stands for the mode prediction, $Y_{obs,i}$ for the associated observed data set, and n for the number of non-missing data points associated with the mode prediction.

The coefficient of determination (R^2) indicates the proportion of variance that the model can explain. It can be determined as follows:

$$R^2 = \left[\frac{n\sum_{i=1}^{n} Y_{obs,i}Y_{pre,i}-(\sum_{i=1}^{n} Y_{obs,i})(\sum_{i=1}^{n} Y_{pre,i})}{\sqrt{\left[n\sum_{i=1}^{n} Y^2_{obs,i}-(\sum_{i=1}^{n} Y_{obs,i})^2\right]\times\left[\sum_{i=1}^{n} Y^2_{pre,i}-(\sum_{i=1}^{n} Y_{pre,i})^2\right]}}\right]^2 \quad \ldots(6)$$

The statistical performance evaluation criteria, such as RMSE and R^2, are global statistics that do not provide any insight into the error distribution. As a result, other performance evaluation criteria, such as mean absolute error (MAE), were applied to measure the accuracy of the ANN models constructed for this investigation. The MAE not only illustrates the distribution of the errors made in the forecast, but it also demonstrates the performance index in predicting removal efficiency. This is because the MAE gives both of these things. The following equation can be used to determine MAE:

$$MAE = \frac{1}{n}\sum_{i=1}^{n}\left|Y_{obs,i} - Y_{pre,i}\right| \quad \ldots(7)$$

RESULTS AND DISCUSSION

Pre-Processing of Data

Seventy nine data sets in this investigation were gathered through batch experiments with varying adsorbent dosages, contact times, and initial Cr(VI) ion concentrations. Experimental data points were randomly split into training, validation, and testing subsets to create an ANN model for forecasting the percentage of Cr(VI) ions removed by WTAC from aqueous solutions. About 70% of the data went to the training set. The remaining 15% and 15% went to the validation and testing sets, which got 55, 12, and 12 data points, respectively.

Table 2: The basic statistics of the ANN model variable.

Input Parameter	Unit	Min.	Max.	Avg.	Std.
Doges	g	0.2	0.8	0.50	0.21
Concentration	$mg.L^{-1}$	10	100	58.86	31.21
Time	Min	10	360	175.31	96.99
Temp.	^oC	30	50	36.83	7.43

The neural network can recognize patterns present in the data by using the training data, which is the largest set, to adjust the network weights. The testing data is employed to assess the network's quality. The trained network's performance and generalizability are checked one last time using validation data. Table 2 presents the essential statistical information regarding the variables used in the investigation.

Before training the network, input and output variables were normalized to fall between 0.1 and 0.9 to avoid numerical overflows caused by extreme weight values. Here is the equation for normalization:

$$X_i = \frac{(x - x_{min})}{(x_{max} - x_{min})} + 0.1 \quad \ldots(8)$$

Where x_{max} and x_{min} represent the maximum and minimum possible values in the database, respectively, and Xi represents the value of x after it has been normalized.

ANN Architecture Design

The architecture of the AAN considerably affects the overall performance of ANN models. To develop the most effective architecture for an ANN model, the network architecture design must consider two essential characteristics: layering and transfer function. With these parameters, the best training algorithm and number of neurons to use in the hidden layer can be chosen.

Table 3: List of different training algorithms of ANN.

ANN Algorithms	EPOCH	RMSE	R^2
TRINLN	128	8.597	0.967
TRAINBGF	10	6.039	0.984
TRAINCGB	56	5.894	0.985
TRAINCGF	132	6.566	0.981
TRAINCGP	1	6.364	0.982
TRAINGDA	12	6.757	0.980
TRAINGDX	104	8.341	0.969
TRAINLM	8	6.214	0.983
TRAINOSS	39	7.518	0.975
TRAINSCG	62	6.110	0.983

The most effective training algorithm can be identified by analyzing and comparing several different training algorithms. The training algorithms used a three-layer ANN with a linear transfer function (purelin) in the output layer, a tangent sigmoid function (tansig) in the hidden layer, and 10 neurons in each layer. Table 3 displays the results of ANN model evaluations using each available training algorithm. As shown in Table 3, the RMSE values obtained by the traincgb were the lowest, and the R^2 values were the highest, coming in at 5.894 and 0.9885, respectively. Because of this, it was selected as the most effective algorithm for training. This algorithm was followed by the training and traincg functions, which had RMSE of 6.039 and 6.110, respectively. When utilized as a training algorithm, alternative algorithms like trainln, traincgf, and traingda produced more errors than the traincgb.

After figuring out the best training algorithm for the ANN model, the next step is optimal design, which involves

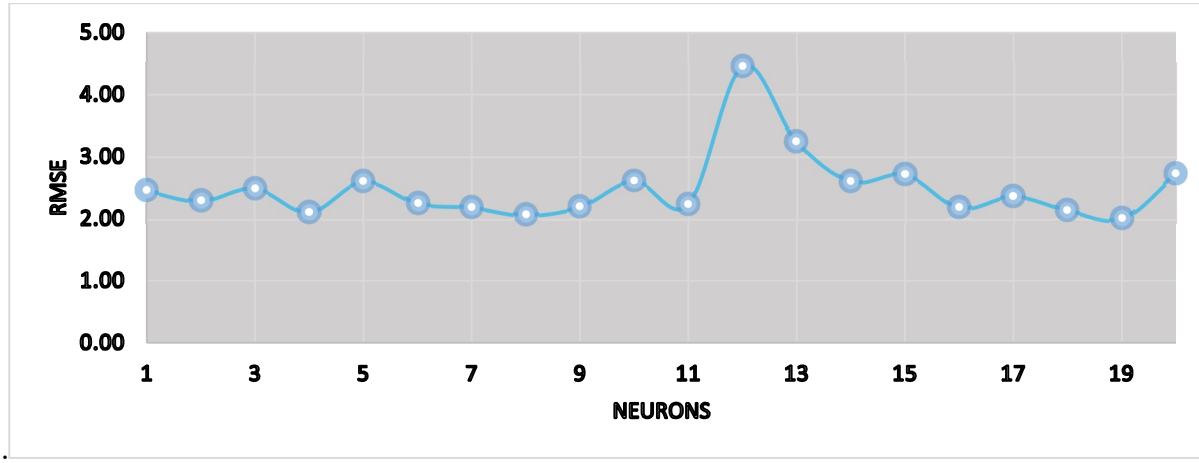

Fig. 5: Variation of RMSE with neurons.

choosing the right number of neurons to use in the hidden layer for further analysis. It can be done by varying the neurons in the hidden layer. Initially, the hidden layer only used two neurons for the guessing process. However, as shown in Fig. 5, the number of neurons in the hidden layer gradually increased from two to twenty.

Fig. 5 shows that the network output a wide range of RMSE and local minimum/maximum values as the number of neurons is enhanced. The lowest RMSE value for the eight hidden neurons was attained in every trial. The smallest RMSE value for a neural network architecture with 8 hidden neurons was 2.06. As a result, the optimal number of neurons was established to be 8 in hidden layers.

Final Selected ANN Model Results

The optimal ANN topology for forecasting Cr(VI) ion adsorption efficiency by WTAC was determined to be 4-8-1 during network architecture design. Table 4 shows the performance of the artificial neural network (ANN) model and the best ANN parameter combination for this structure.

In summary, Fig. 6 illustrates the optimal three-layer ANN topology, comprising a four-neuron input layer, an eight-neuron hidden layer with a tangent sigmoid (tansig) transfer function, and a single-neuron output layer.

A linear relationship between the observed and predicted outputs of the final selected ANN model can be seen in training, validation, and testing over the full dataset. As shown in Fig. 7, the regression plot was obtained for the best ANN model 4-8-1. The good accuracy and fitting abilities of the ANN model are demonstrated by the large R-value of 0.977 for the entire data set. The lower R-value of 0.91014 shown in the testing data may be due to the limited sample size used in this investigation. Expected values based on the best ANN model 4-8-1 are displayed in Table 4.

An evaluation of the ANN model's efficacy was conducted by contrasting the error function with respect to the validation data. The training procedure ends once the validation error has decreased to a certain level. The outcome is predicted, and ANN validates the experimental data. The MSE for the optimized ANN model is shown against the epoch number in Fig. 8. Overfitting was avoided, and the least-error weights and biases were recovered by stopping training after 61 epochs, as shown in Fig. 8. Specifically, the little circle at epoch 61 on the graph represents the highest validation performance.

Table 4: Artificial Neural network (ANN) model's performance.

ANN Structure	Algorithm	Transfer function		Assessment Criteria		
		Hidden Layer	Output layer	RMSE	MAE	R^2
4-8-1	Treincbg	tansing	purelin	2.384	1.630	0.977

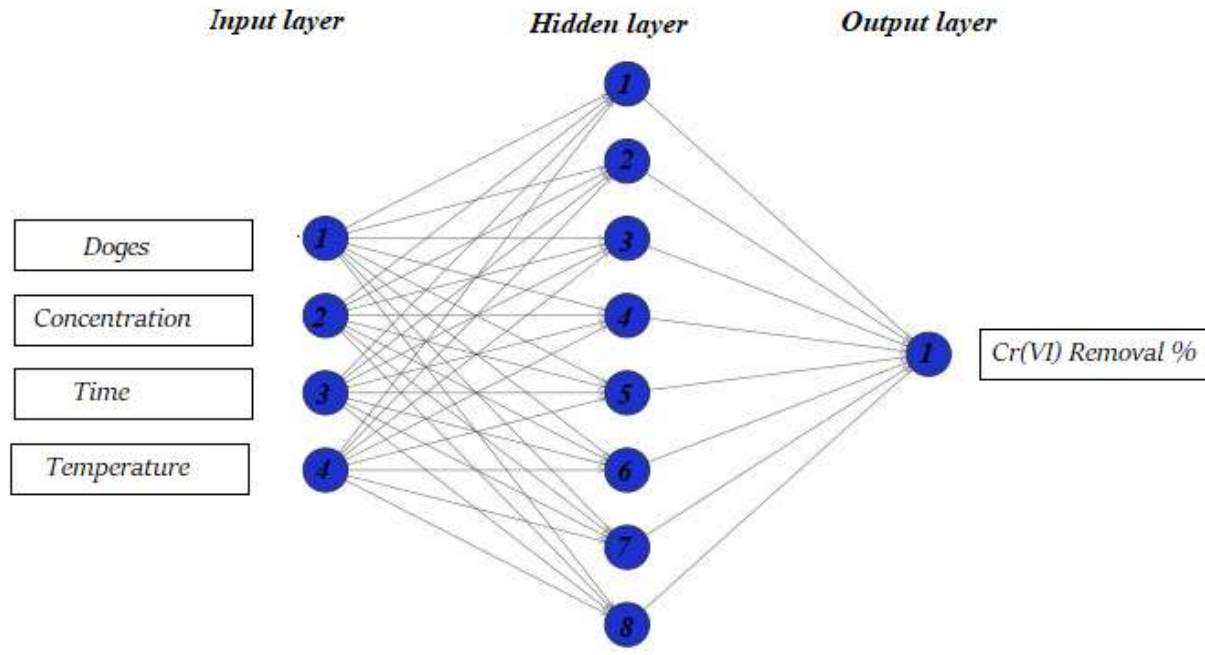

Fig. 6: ANN topology (4-8-1) for Cr(VI) adsorption efficiency.

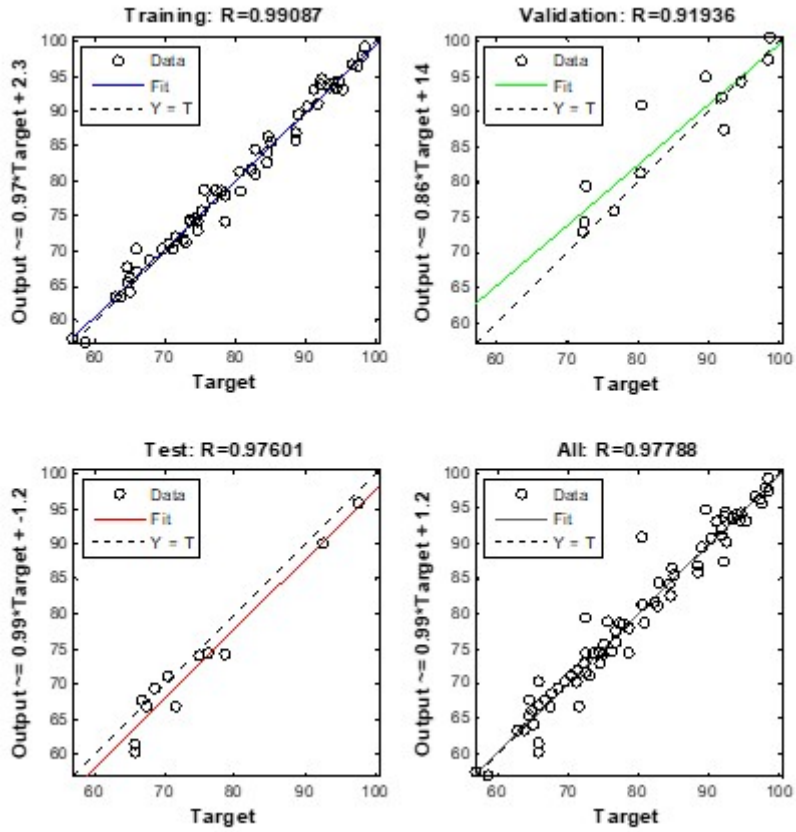

Fig. 7: Regression plots of ANN model for Cr(VI) adsorption efficiency.

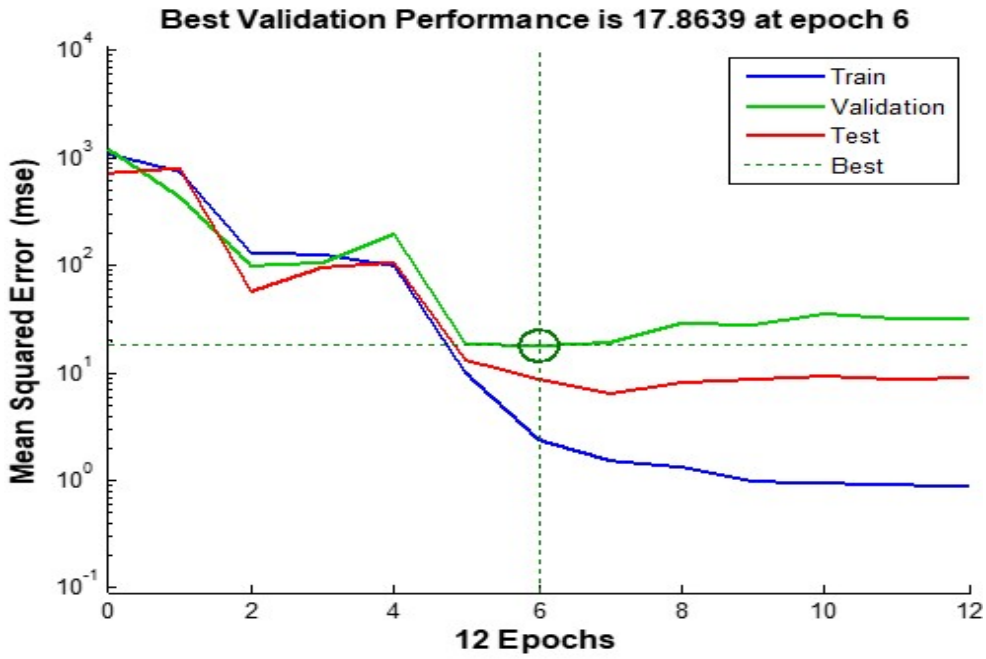

Fig. 8: MSE plot of ANN performance for train, validation, and test data.

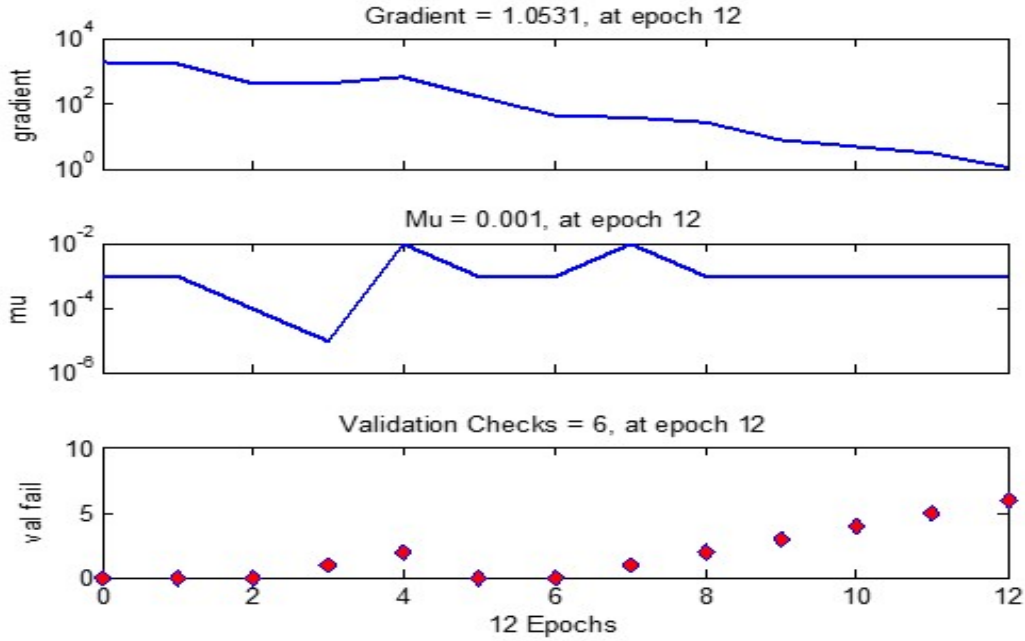

Fig. 9: ANN Training State (Gradient, mu, and validation check profiles).

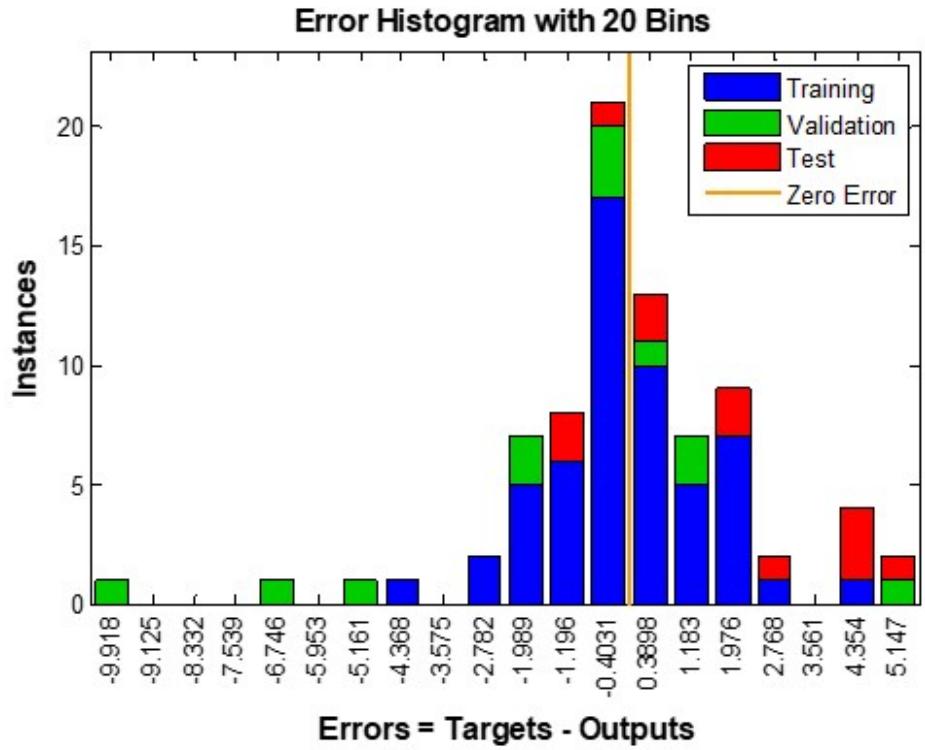

Fig. 10: Histogram of error.

The validation check, also known as Mu, and the gradient profile of the ANN model are depicted in Fig. 9. When the gradient value reached 1.0531. The training was terminated. As shown in Fig. 9, the mu value for the seventh period was 0.001. Additionally, the varying validation checks show no need to evaluate the validity of the data set used in the current investigation.

After projecting the errors for each data point, a 20-bin error histogram is generated and displayed in Fig. 10. Fig. 10 shows that the largest error possible was 10.31, and the smallest error possible was 0.003. The fact that 4 of the observations had zero or tiny errors and the deviations are concentrated closer to the zero error line demonstrates the correctness and reliability of the ANN model developed. However, the limited dataset used means that the amount of errors that significantly depart from the mean is still manageable.

CONCLUSION

The primary aim of this research was to develop an ANN model for the Cr(VI) ion adsorption efficiency of WTAC in batch adsorption tests with four different process parameters (adsorbent dosage, initial concentration of Cr(VI) ions, contact time, and temperature). WTAC was developed using the carbonization of waste tires at 400 °C, which was subsequently activated using a thermal and chemical method. WTAC's FTIR peak at 3415.02 cm indicates the presence of a hydroxyl group.

A three-layer ANN with different training algorithms and hidden layers with different numbers of neurons was developed to predict the adsorption efficiency of the Cr(VI) ion. All algorithms were evaluated at 10 neurons in a hidden layer. The best training algorithm was determined to be CGB of Powell-Beale restarts (traincgb), with RMSE of 5.894 and R^2 of 0.985. It was determined that 8 neurons in the hidden layer are the optimal number for traincgb, with RMSE 2.06. The ANN model's correlation coefficient is 0.977, indicating that it accurately predicted experimental data and could make a reliable prediction on the adsorption efficiency of the Cr(VI) ion.

REFERENCES

Aksu, Z. 1996. Investigation of biosorption of chromium(vi) on cladophora crispata in a two-staged batch reactor. Environ. Technol., 7(2): 215-20.

Basso, M.C., Cerrella, E.G. and Cukierman, A.L. 2002. Activated carbons developed from a rapidly renewable biosource for the removal of cadmium(II) and nickel(II) ions from dilute aqueous solutions. Ind. Eng. Chem. Res., 41(2): 180-89.

Bereket, G., Ayşe, Z., Aroğuz, R. and Mustafa, Z.O. 1997. Removal of Pb(II), Cd(II), Cu(II), and Zn(II) from aqueous solutions by adsorption on bentonite. J. Coll. Interf. Sci.,187(2): 338-43.

Chakravarti, A.K., Chowdhury, S.B. and Mukherjee, D.C. 2000. Liquid membrane multiple emulsion process of separation of copper(II) from wastewaters. Coll. Surf. A Physicochem. Eng. Aspects, 166(1-3): 7-25.

Chen, H. and Kim, A.S. 2006. Prediction of permeate flux decline in crossflow membrane filtration of colloidal suspension: A radial basis function neural network approach. Desalination, 192(1-3): 415-28.

Das, A.K. 2004. Micellar effect on the kinetics and mechanism of chromium(VI) oxidation of organic substrates. Coord. Chem. Rev., 248(1-2): 81-99.

Dodbiba, G., Josiane, P. and Toyohisa, F. 2015. Biosorption of heavy metals. Microbiol. Minerals Metals Mater. Environ., 409-26.

El-Sikaily, A., Ahmed El, N., Azza, K. and Ola, A. 2007. Removal of toxic chromium from wastewater using green alga *Ulva lactuca* and its activated carbon. J. Hazard. Mater., 148(1-2): 216–228.

Fagundes-Klen, M.R. 2007. Equilibrium study of the binary mixture of cadmium-zinc ions biosorption by the *Sargassum filipendula* species using adsorption isotherms models and neural network. Biochem. Eng. J., 34(2): 136-146.

Gómez, V. and Callao, M.P. 2006. Chromium determination and speciation since 2000. TrAC - Trends Anal. Chem., 25(10): 1006-1015.

Gontarski, C.A., Rodrigues, P.R., Mori, M. and Prenem, L.F. 2000. Simulation of an industrial wastewater treatment plant using artificial neural networks. Comp. Chem. Eng., 24(2-7): 1719-1723.

Guadix, A., Jose, E.Z., Carmen Almecija, M. and Guadix, E.M. 2010. Predicting the flux decline in milk crossflow ceramic ultrafiltration by artificial neural networks. Desalination, 250(3): 1118-1120.

Gupta, V.K. 2003. Removal of cadmium and nickel from wastewater using bagasse fly ash - a sugar industry waste. Water Res., 37(16): 4038-44.

Jiao, C. and Ding, Y. 2009. "Foam Separation of Chromium (VI) from Aqueous Solution. Journal of Shanghai University, 13(3): 263-66.

Kannan, N. and Rengasamy, G. 2005. Comparison of cadmium ion adsorption on various activated carbons. Water Air Soil Pollut., 163(1-4): 185-201.

Kashaninejad, M., Dehghani, A.A. and Kashiri, M. 2009. Modeling of wheat soaking using two artificial neural networks (MLP and RBF). J. Food Eng., 91(4): 602-607. http://dx.doi.org/10.1016/j.jfoodeng.2008.10.012.

Kongsricharoern, N. and Polprasert, C. 1996. Chromium removal by a bipolar electrochemical precipitation process. Water Sci. Technology, 34(9): 109-16. http://dx.doi.org/10.1016/S0273-1223(96)00793-7.

Kowalski, Z. 1994. Treatment of chromic tannery wastes. J. Hazard. Mater., 37(1): 137-41.

Li, H. 2008. A novel technology for biosorption and recovery of hexavalent chromium in wastewater by bio-functional magnetic beads. Bioresour. Technol., 99(14): 6271-79.

Libotean, D. 2009. Neural network approach for modeling the performance of reverse osmosis membrane desalting. J. Membr. Sci., 326(2): 408-419.

Manchón-Vizuete, E. 2005. Adsorption of mercury by carbonaceous adsorbents prepared from rubber of tire wastes. J. Hazard. Mater., 119(1-3): 231-38.

Meegoda, J.N. 2000. Emediation of chromium contaminated oils: Practice periodical of hazardous, toxic. Radioact. Waste Manag., 4(1): 7-15.

Monser, L. and Adhoum, N. 2002. Modified activated carbon for the removal of copper, zinc, chromium, and cyanide from wastewater. Sep. Purif. Technol., 26(2-3): 137-146.

Ngah, W.S.,Wan, S., Ghani, A.B. and Kamari, A. 2005. Adsorption behavior of Fe(II) and Fe(III) ions in aqueous solution on chitosan and cross-linked chitosan beads. Bioresour. Technol., 96(4): 443-450.

World Health Organization (WHO). 2020. Chromium in Drinking Water: A Background Document for Development of World Health Organisation Guidelines for Drinking Water. WHO, Geneva, pp. 1-30.

Pai, T.Y. 2007. Grey and neural network prediction of suspended solids and chemical oxygen demand in hospital wastewater treatment plant effluent. Comp. Chem. Eng., 31(10): 1272-1281.

Prakash, N., Manikandan, S.A., Govindarajan, L. and Vijayagopal, V. 2008. Prediction of biosorption efficiency for the removal of c opper(II) using artificial neural networks. J. Hazard. Mater., 152(3): 1268-1275.

Qiao, J.F., Xin, G. and Wen, J.L. 2020. An online self-organizing algorithm for feedforward neural network. Neural Comp. Appl., 32(23): 17505-17518. https://doi.org/10.1007/s00521-020-04907-6.

Religa, P., Kowalik, A. and Gierycz, P. 2011. Application of nanofiltration for chromium concentration in the tannery wastewater. J. Hazard. Mater., 186(1): 288-292. http://dx.doi.org/10.1016/j.jhazmat.2010.10.112.

Rowley, A.G., Husband, F.M. and Cunningham, A.B. 1984. Mechanisms of metal adsorption from aqueous solutions by waste tyre rubber. Water Res., 18(8): 981-984.

Sadrzadeh, M., Toraj, M., Javad, I. and Norollah, K. 2009. Neural network modeling of Pb^{2+} removal from wastewater using electrodialysis" Chem. Eng. Process. Intensif., 48(8): 1371–1381.

Sahoo, G.B. and Ray, C. 2006. Predicting flux decline in crossflow membranes using artificial neural networks and genetic algorithms. J. Membr. Sci., 283(1-2): 147-157.

Selomulya, C., Meeyoo, V. and Amal, R. 1999. Mechanisms of Cr(VI) removal from water by various types of activated carbons. J. Chem. Technol. Biotechnol., 74(2): 111-22.

Taty-Costodes, V. Christian, H.F., Catherine, P. and Alain, D. 2003. Removal of Cd(II) and Pb(II) ions, from aqueous solutions, by adsorption onto sawdust of *Pinus sylvestris*. J. Hazard. Mater., 105(1-3): 121-142.

Tiravanti, G., Petruzzelli, D. and Passino, R. 1997. Pretreatment of tannery wastewaters by an ion exchange process for Cr(III) removal and recovery. Water Sci. Technol., 36(2-3): 197-207. http://dx.doi.org/10.1016/S0273-1223(97)00388-0.

Veglio, F. and Beolchini, F. 1997. Removal of Metals by Biosorption: A Review. Hydrometallurgy, 44(3): 301-316.

Yetilmezsoy, K. and Demirel, S. 2008. Artificial neural network (ANN) approach for modeling Pb(II) adsorption from aqueous solution by Antep Pistachio (Pistacia Vera L.) Shells." Journal of Hazardous Materials, 153(3): 1288-1300.

Zhou, X. 1993. A process monitoring/controlling system for the treatment of wastewater containing chromium(VI).Water Res., 27(6): 1049-1054.